The solution to DEM resolution effects and parameter inconsistency by using scale-invariant TOPMODEL

Jing Xu, Liliang Ren, Fei Yuan and Xiaofan Liu

ABSTRACT

The parameter calibration of TOPMODEL is influenced by digital elevation model (DEM) resolution because of the utilization of scale-dependent topographic index representing hydrologic similarity. The downscaled DEM from the coarse-resolution DEM and the resolution factor are applied to remove the DEM scale effects on the upslope area. Meanwhile, a fractal method is introduced as an approach to account for the effect of DEM resolution on slope. A significant improvement on the estimation of slope directly from the coarse-resolution data is made by applying fractal parameters that are computed from the standard deviation of elevation and the topographic complexity index in a 3×3 window of the DEM to account for local variability in the surface. The method to downscale the topographic index distribution is then coupled with the TOPMODEL to develop the scale-invariant TOPMODEL and is applied to perform streamflow simulation in the context of different DEM resolutions in the Zishui catchment. Results show that the calculated hydrograph based on the DEM data at 900 and 1,800 m resolution is consistent with that based on the DEM data at 100 m resolution when the same parameter set is used.

Key words | fractal, scale, TOPMODEL, topography, transform

Jing Xu (corresponding author)
State Key Laboratory of Pollution Control and Resource Reuse and Department of Hydrosciences,
Nanjing University,
Nanjing 210093,
China
E-mail: *xujing@nju.edu.cn*

Liliang Ren
Fei Yuan
Xiaofan Liu
State Key Laboratory of Hydrology, Water Resources and Hydraulic Engineering,
Hohai University,
Nanjing 210098,
China

INTRODUCTION

Topography defines the effects of gravity on the movement of water and sediments in a catchment, therefore digital elevation models (DEMs) play a considerable role in hydrologic simulation, soil-erosion and landscape-evolution modeling (Zhang *et al.* 1999). Many studies have indicated that as the DEM resolution decreases, the slope tends to decrease, whereas the specific catchment area and topographic index are usually augmented (Wolock & Price 1994; Zhang & Montgomery 1994; Quinn *et al.* 1995). Gallant & Hutchinson (1996) found that the DEM spatial resolution affects topographic characteristics through terrain discretization and smoothing. Wolock & McCabe (2000) demonstrated that most of the difference between high- and low-resolution DEMs is mainly attributed to a terrain discretization effect that arises from dividing the terrain into different numbers of grid cells. It means that downscaling of the DEM scale to appropriate size can reduce the effects of DEM resolution on topographic characteristics calculation.

At present, the distributed hydrologic models are built on the basis of DEM data. Despite the enormous capacity of today's information technologies, the complexity of the Earth's surface is such that the most voluminous descriptions are still only coarse generalizations of what is actually present (Goodchild 2001). This situation implies the self-evident need for continued and sustained research on scale issues. In order to develop more physically realistic distributed models, the dependence of models on calibrated 'effective parameters' with physically realistic process descriptions should be replaced. As the spatial extent is expanded beyond point experiments to larger watershed regions, the direct extension of the models valid at the small scale requires an estimation of the distribution of model parameters and process computations over the heterogeneous land surface (Pradhan *et al.* 2004). If a distribution of a set of spatial variables required for a given hydrological model can be described by a joint

doi: 10.2166/nh.2011.130

density function, then the fractal method and geographical information system (GIS) may be evaluated as a tool for estimating this function. According to Huang & Turcotte (1989), the Earth topography obeys fractal statistics and the mean fractal dimension (D) is 1.52. This fact implies that there should be a linkage between the observed topography and the scale of measurement. If these relations can be translated into effective hydrological models, the solution to the scale issue of topographic characteristics may be found. Undoubtedly, it is useful for prediction in ungauged basins of developing countries where only coarse-resolution DEM data are available.

In this paper, we focus on the effect of DEM resolution on slope, upslope contributing area, and propose a method to downscale the topographic index of TOPMODEL by incorporating scaling laws that can bridge the gap between scaling issues. Then the method of scale transformation is coupled with TOPMODEL to develop the scale-invariant TOPMODEL. The model is applied in flood event simulation in the Zishui watershed to confirm the effectiveness of solution to scale issues.

TERRAIN-DISCRETIZATION AND SMOOTHING EFFECTS OF DEM RESOLUTION

The SRTM3 data covering the Zishui watershed within 25°–30° N and 110°–115° E are selected. The digital elevation drainage network model (DEDNM) was used to process the DEM data including depression filling, extraction of slope and contributing area (Martz & Garbrecht 1992).

In terms of confirming the contribution of terrain discretization, 3-arcsecond DEMs for 57 locations in the Zishui River basin in China were used to compute topographic characteristics such as slope, upslope contributing area and topographic index. The DEM data covering each location contains 500 rows and 500 columns. Three kinds of DEM data were used to investigate and separate the terrain-discretization and smoothing effects. Those data were labeled as the orig100-m, 1,000-m and new100-m DEMs. The orig100-m DEM was extracted directly from a larger elevation image at a resolution of 3 arcseconds by using the ENVI software. The 1,000-m DEM was generated by resampling the orig100-m DEM at every 10th point. The new 100-m DEM was created by bilinearly interpolating the 1,000-m DEM to 100 m resolution using the GIS software ARCGIS.

The topographic characteristics calculated from the orig100-m, 1,000-m and new100-m DEMs were compared to examine the effects of DEM resolution. The terrain-discretization effect of DEM resolution was isolated by comparing the topographic characteristics computed from the 1,000-m and new100-m resolution DEMs. The 1,000-m and new100-m DEMs have the same amount of terrain information but different levels of terrain discretization. The terrain-smoothing effect was isolated by comparing the topographic characteristics computed from the orig100-m and new100-m DEMs. The orig100-m and new100-m DEMs have the same level of terrain discretization but different amount of terrain information. The combined discretization and smoothing effects were determined by comparing the orig100-m and 1,000-m DEMs. Both of them have different levels of terrain discretization and smoothing (Wolock & McCabe 2000).

As shown in Figure 1, the distance between the one-to-one line and the new100-m points is defined as the smoothing effect, and the distance from the 1000-m points to the new100-m points is described as the discretization effect. The result is different from the previous research of Wolock & McCabe (2000) (Xu *et al.* 2008). The effects of DEM resolution on slope mainly result from terrain smoothing, and the terrain discretization accounts for most of the difference between upslope contributing area values calculated from 100 m and 1,000 m DEM. The effects of discretization and smoothing are almost same on topographic index.

In Table 1, the discretization effect is the 1,000-m value minus the new100-m value. The smoothing effect is the new100-m minus 1,000-m value. The discretization plus smoothing effects is the 1,000-m value minus the orig100-m value. The same conclusion can be drawn from Figure 1.

It can be concluded that disaggregation of DEM into appropriate size can improve the estimates of upslope contributing area and slope.

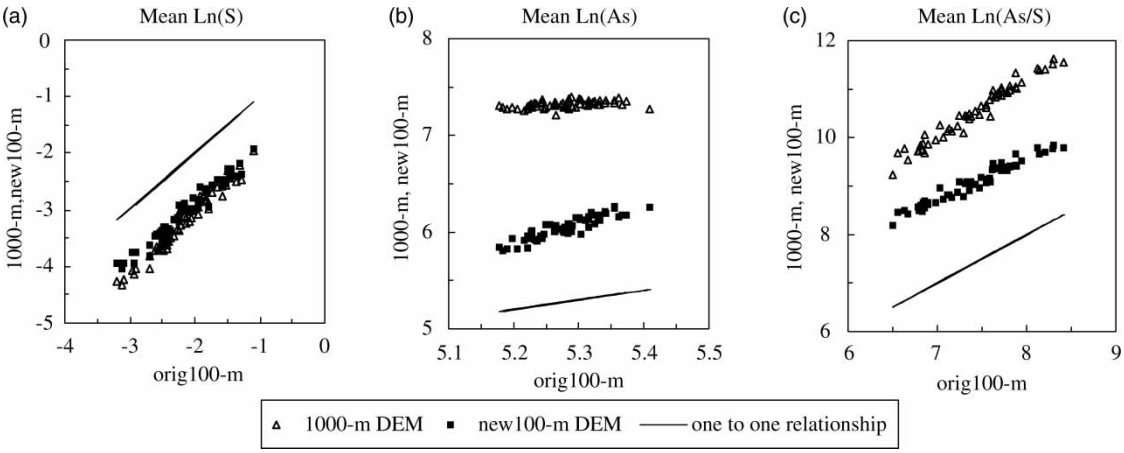

Figure 1 | Comparison of mean upslope area (ln(A_s)), mean slope (ln(S)) and mean topographic index (lnA_s/S)) computed from 100-m and 1,000-m DEMs for 57 locations in the Zishui watershed.

Table 1 | Discretization and smoothing effects of DEM resolution on mean values of upslope area, slope and topographic index

Topographic characteristic		ln(A_s)	ln(S)	ln(A_s/S)
Discretization effect	Minimum	1.01	–0.32	1.04
	Median	1.28	–0.17	1.48
	Maximum	1.48	–0.018	1.76
Smoothing effect	Minimum	0.61	–1.14	1.37
	Median	0.76	–0.88	1.68
	Maximum	0.91	–0.69	1.93
Discretization plus smoothing effects	Minimum	1.86	–1.33	2.73
	Median	2.04	–1.08	3.14
	Maximum	2.13	–0.81	3.46

EFFECTS OF DEM RESOLUTION ON HYDROLOGIC SIMULATION

Introduction of TOPMODEL

TOPMODEL is a semi-distributed watershed model proposed by Beven & Kirkby (1979). This model is based on topography and simulates streamflow generation according to the variable-source-area concept. In TOPMODEL, streamflow will be produced when the land surface areas become saturated because of the rise in water table during precipitation events. The variable-source-area concept considers that streamflow is composed of overland flow and base flow, and that it is usually produced only over a small portion of the total watershed area called the source area (Wolock & Mccabe 1995).

One fundamental equation in TOPMODEL states that the saturated deficit at any location x is determined by the watershed average saturation deficit ($\overline{S}$) and the difference between the mean of the ln(A_s/tan β) distribution (λ) and the value of ln(A_s/tan β) at location x:

$$S_x = \overline{S} + m\left[\lambda - \ln\left(\frac{A_s}{\tan\beta}\right)\right] \quad (1)$$

where m is a decay parameter. Equation (1) shows that values of ln(A_s/tan β) relate directly to the likely distribution of variable source areas within watershed (Quinn *et al.* 1995). Locations in the watershed with larger ln(A_s/tan β) are most likely to be saturated and to produce overland flow.

The influence of DEM resolution on TOPMODEL performance

The topographic index is obviously influenced by DEM resolution. As description above, TOPMODEL utilizes the topographic index to represent hydrologic similarity in runoff generation, so the DEM resolution can also affect its application performance. In Figure 2, the 100 m DEM is derived from the SRTM3 data, and the 300, 900 and

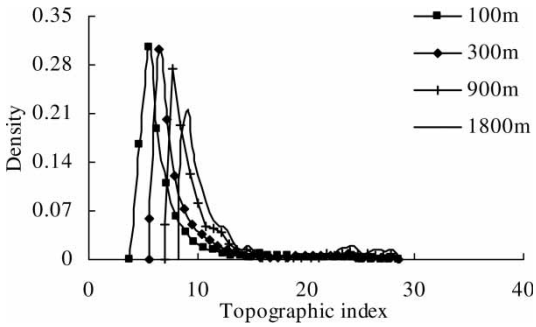

Figure 2 | Comparison of the density functions of the topographic index at four different DEM resolutions in the study basin.

1,800 m DEM is obtained from 100 m DEM by aggregation. The curves show the density function of the topographic index at four different DEM resolutions in the contributing area controlled by Xinning hydrologic station in the Zishui watershed (2,456 km^2) without taking into account the scale effect. The distinct swift of topographic index density function towards the higher value could be easily observed as the resolution of DEM gets coarser. As shown in Figure 3, the effects of DEM resolution cause an increase in runoff volume and flood peak because of the larger topographic index calculated from the coarser DEMs.

Topographic index is scale dependent which leads identified parameter values to be dependent on DEM resolution. This situation makes it difficult to use model parameter values identified with different resolution models. If only coarse DEM data are available, we can readily imagine the blunder in predicting ungauged basins. To overcome the problem, a scale-invariant model of the topographic index is proposed.

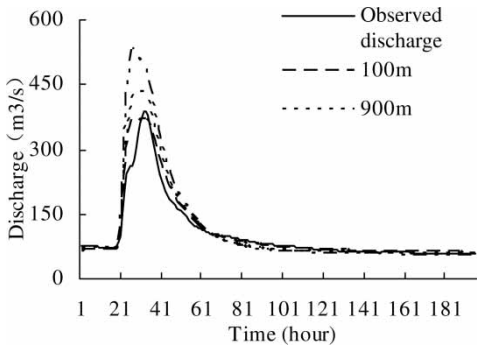

Figure 3 | Comparison of runoff simulation performance of No. 800612 flood at three different DEM resolutions in the study basin.

THE ESTABLISHMENT OF SCALE-INVARIANT TOP

The development of scale-invariant topmodel

Based on the disaggregated DEM data from the coarse DEM, the resolution factor is introduced to account for the scale effect in up slope contributing area, and a fractal method is applied to account for the scale effect on slopes. Then, the scale-invariant model of the topographic index distribution is constructed. Coupling the downscaled topographic index in TOPMODEL to develop the scale-invariant TOPMODEL for runoff simulation under different DEM scales.

Resolution factor

Any upslope contributing areas smaller than the grid area of the DEM resolution used are completely lost. Thus, a portion of the upslope contributing area that can be well defined by a finer DEM resolution gets completely filtered out if that portion of the upslope catchment area is less than the grid area of the coarse-resolution DEM used (Pradhan *et al.* 2006). For example, at 100 m DEM resolution, the upslope area of most DEM grids is less than 1 km^2 at 1,000 m DEM resolution and there is no grid having an upslope catchment area less than 1 km^2. The loss of the smaller upslope area causes the topographic index distribution from coarse resolution DEM to move swiftly towards higher values (see Figure 2).

The smaller contributing area can be achieved due to the finer grid resolution. Therefore, we introduce the Resolution Factor R_f concept of topographic index (Pradhan *et al.* 2004):

$$R_f = \frac{W_{low}}{W_{target}} \quad (2)$$

where W_{low} is the grid size of the coarse resolution DEM and W_{target} is the grid size of the target resolution DEM.

Fractal method for scaled steepest slope

The underestimation of slopes by using the coarse resolution DEMs can seriously affect the accuracy of hydrologic and geomorphological models. To scale the local slope, we

followed the fractal theory in topography and slope proposed by Klinkenberg & Goodchild (1992) and Zhang *et al.* (1999) and developed a modified fractal method for slope.

The variogram technique (statistical variation of the elevations between samples varies with the distance between them) can be used to calculate the fractal dimension in a region when the log of the distance between samples is regressed against the log of the mean squared difference in the elevations for that distance.

According to the variogram technique, the relationship between the elevations of two points and their distance can be converted to the following formula:

$$(E_p - E_q)^2 = kd^{4-2D} \tag{3}$$

where E_p and E_q are the elevations at points p and q, d is the distance between p and q, k is a constant and D is fractal dimension. So,

$$\frac{E_p - E_q}{d} = \alpha d^{1-D} \tag{4}$$

where $\alpha = \pm k^{0.5}$ is a constant. Because the value $(E_p - E_q)/d$ is actually the surface slope, it can be assumed that the slope value S is associated with its corresponding scale (grid size) d by the equation:

$$S = \alpha d^{1-D}. \tag{5}$$

This relationship implies that if topography is fractal, then slope will also be a function of the scale of measurement. However, it is impossible to predict the spatial patterns of slopes due to the single value of the fractal dimension and the coefficient in the fractal slope equation for the whole DEM. It is reasonable to suppose that different kinds of terrain might have characteristic topography that can be expressed in terms of different values of α and D (Barenblatt *et al.* 1984; Fox & Hayes 1985; Klinkenberg 1992). In order to use Equation (5) to calculate local slope at a specified finer scale (d) it is necessary to develop a method for calculating the local fractal parameters from the coarse-resolution data.

In the light of the assumptions proposed by Zhang *et al.* it can be concluded that the coefficient α and fractal dimension D of Equation (5) are mainly controlled by standard deviation (σ) of the elevation of the sub-regions in a DEM. In order to derive the regression equations, this study considered the smallest subarea (window) to be composed of 3×3 pixels. Hence, elevations of nine neighboring grids in the DEM were taken to obtain the standard deviation of the elevation for subareas. The regression equations for α and D separately with the standard deviation (σ) of the elevation were brought out, but the correlation coefficients (r^2) for the two regression equations were only 0.34 and 0.135.

In order to improve the reliability of regression equations, the terrain complexity index (TCI) was introduced to reveal the complexity and variation of true land surface. In a 3×3 DEM window, eight dihedral angles can be formed according to the elevation (Z coordinates) and the location (X, Y coordinates) of the grid cell. TCI uses the mean values of eight dihedral angles. The value of each dihedral angle can be calculated by the following equation:

$$\cos(\varphi) = \frac{|a_1a_2 + b_1b_2 + c_1c_2|}{\sqrt{(a_1^2 + b_1^2 + c_1^2) \times (a_2^2 + b_2^2 + c_2^2)}} \tag{6}$$

where (a_1, b_1, c_1) is normal vector of the first plane, (a_2, b_2, c_2) is the normal vector of the second plane, and the angle is in rad. When the TCI is introduced, the regression equations can be stated as follows:

$$\alpha = 0.872 - 0.02 \times \sigma + 4.893 \times \mathrm{TCI} + 8.733 \times S_{\mathrm{low}} \tag{7}$$

with $r^2 = 0.493$, $n = 900$, $F = 290.095$ and $p < 1 \times 10^{-5}$; and

$$D = 2.055 + 0.733 \times \mathrm{TCI} - 0.182 \times \ln(\sigma) \tag{8}$$

with $r^2 = 0.801$, $n = 900$, $F = 1806.781$ and $p < 1 \times 10^{-5}$, where S_{low} is the slope of coarse DEM data. In order to obtain these regression equations, the 100 m resolution DEM covering the Zishui watershed (2,456 km^2) is used. The DEM is composed of 1620 rows and 1620 columns

and divided into 900 subareas. Each subarea has 54 rows and 54 columns. The variables, such as σ, α, D and TCI, are computed to derive the regression equations. There is a little defect with Equation (7) because of the limited extension. When the elevation varies remarkably, it means there will be a large value of σ, which will make $\alpha < 0$. If this option happens, Equation (7) is replaced by (Pradhan *et al.* 2004):

$$\alpha = \frac{S_{\text{low}}}{d_{\text{low}}^{1-D}}. \tag{9}$$

The local values of TCI and σ can be derived by the 3×3 moving window pixels of the coarse-resolution DEM, and then the slope at target resolution of each grid can be calculated by Equations (5)–(9).

Fractal topographic index

The fractal slope is labeled as S_{f}, and the upslope area at target DEM resolution is labeled as A^*. Then the fractal topographic index at target DEM resolution can be calculated using the following equation:

$$\text{TI} = \ln\left(\frac{A^*}{S_{\text{f}}}\right). \tag{10}$$

The A^* can be computed by the following equation, where A_{s} is the value of the upslope area calculated from the coarse-resolution DEM:

$$A^* = \frac{A_{\text{s}}}{R_{\text{f}}}. \tag{11}$$

Based on the disaggregated DEM, the resolution factor and fractal method are applied to remove the effect of DEM resolution on topographic index calculation.

Coupling the downscaled topographic index in TOPMODEL

100, 900 and 1,800 m DEM are used in this paper. 100 m DEM is regarded as the target resolution DEM, and 900 and 1,800 m DEM are used as coarse-resolution DEMs. First of all, the downscaled resolution for coarse-resolution DEM should be determined. The right disaggregated resolution for 900 and 1,800 m DEM is 300 and 900 m respectively by application of the 'trial-and-error method'. The trial-and-error method is a common method to calibrate parameters. Here the disaggregated resolution is regarded as a parameter which needs calibration. It is evaluated by comparing the scaled topographic index distribution from the coarse-resolution DEM to target resolution by using a downscaling method with the frequency distribution at the target grid-resolution DEM. The disaggregated resolution is determined when the perfect fit appears. Then, regarding the disaggregated DEM as input, the scaled topographic characteristics at target DEM resolutions were derived by introducing the resolution factor and applying the fractal method. Finally, the runoff simulation was performed by the scale-invariant TOPMODEL.

RESULTS AND DISCUSSION

The Zishui catchment (shown in Figure 4), with a total drainage area of 2,456 km^2, is controlled by Xinning hydrological station and is situated in southern China. There are nine rain gauges, and one meteorological station in this basin. 18 flood events were selected for streamflow simulation. In this study, the hydrological parameters were regarded as the inherent characteristics of a given watershed, and calibrated by the SCE-UA algorithm based on the 100 m DEM, as it contains the most abundant terrain information.

Figure 5(a) shows the cumulative frequency curves of slope computed from 100 and 900 m DEM. The obvious decrease in slope distribution can be observed in Figure 5(a) while the DEM resolution becomes coarser. Figure 5(b) shows the comparison of scaled slope distribution function from the 900 m grid-resolution DEM to 100-m DEM resolution by using fractal method and the distribution function of the slope at 100-m DEM. Although the distribution of scaled slope from 900 m DEM to 100 m DEM resolution does not match so well with the distribution of slope at 100 m DEM resolution, it also can be seen that some lost portion of slope with larger values originally

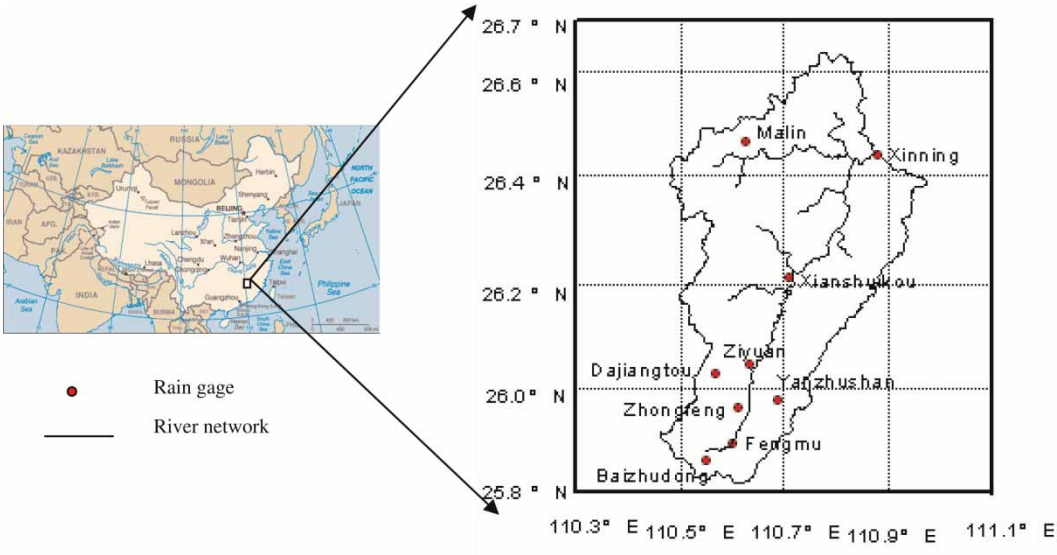

Figure 4 | Location of the Zishui catchment and distribution of meteorological stations and rain gauge stations within the catchment.

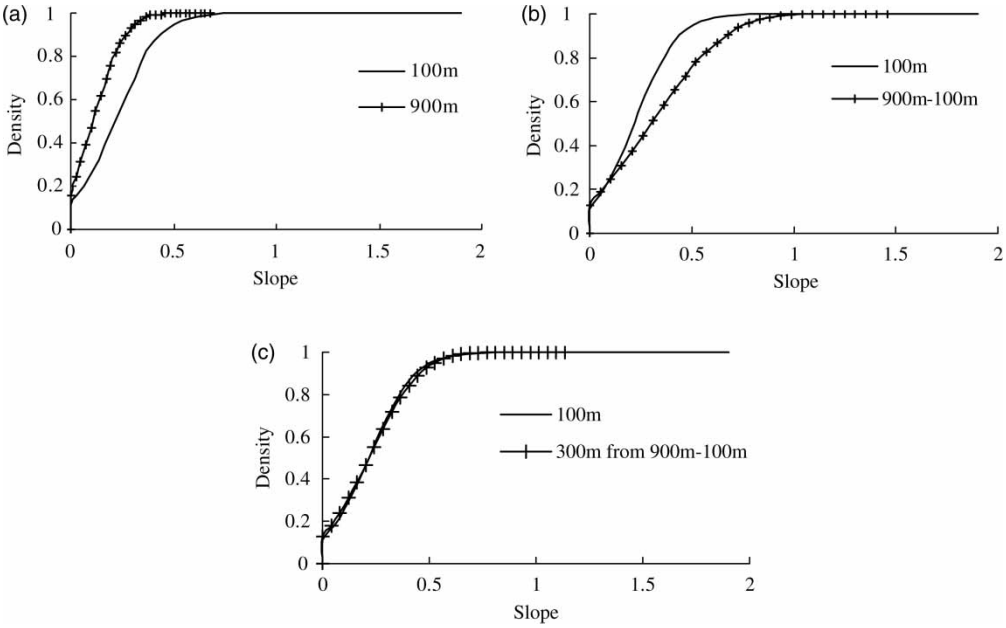

Figure 5 | Cumulative frequency curve of fractal slope with and without downscaling. ('100 m' means the slope computed from the original 100 m DEM. '900 m' indicates the values calculated from the 900 m DEM resampling from 100 m DEM. '300 m from 900 m–100 m' means the fractal slope at the target resolution of 100 m computed from the 300 m DEM which is downscaled from the 900 m DEM.)

defined by the target fine grid-resolution (100 m) DEM value appears again in the distribution of slope from coarse-resolution (900 m) DEM by utilization of downscaling method (Equations (5)–(9)). Figure 5(c) shows the distribution of scaled slope from the disaggregated 300 m DEM to the target resolution of 100 m. The disaggregated DEM data at the resolution of 300 m is originated from 900 m DEM. A close fit of the frequency distribution of

the scaled slope from the disaggregated 300 m DEM to 100 m grid-resolution DEM is shown in Figure 5(c). This situation demonstrates the application of the disaggregated DEM is useful for reducing the effect of DEM resolution on slope calculation.

When the DEM resolution increases, the high-frequency topographic information is lost as the larger sampling dimensions of the grids act as a filter. Figures 6(a) and (b) show the comparison of scaled topographic index frequency distribution from 900 and 1,800 m resolution DEM to the target DEM resolution of 100 m by applying the scale-invariant method and the density function of the topographic index at 100 DEM resolutions. A perfect fit of density functions of scaled topographic indices from the disaggregated DEM to target grid resolution is shown in Figure 6. It can be concluded that the scale-invariant model is a powerful tool to remove the effect of DEM resolution on topographic characteristics calculation.

Figure 7 shows the topographic index map over the study basin. A remarkable difference can be seen between the spatial distribution of the topographic index in Figures 7(a) and (c) for the 100 m resolution DEM and the 1,800 m resolution DEM respectively. As the DEM grid size increases, the grey which denotes the topographic index of small values disappears. This phenomenon implies that the higher-frequency topographic information contained in the topographic index distribution from finer resolution DEM is lost. As shown in Figures 7(d) and (e), through application of the downscaling method, some lost small topographic index values with high-frequency return in the distribution of scale topographic index from coarse grid-resolution DEM. This situation means that higher resolution topographic information can be obtained by downscaling the topographic index distribution from a coarse resolution to a specific fine-resolution DEM.

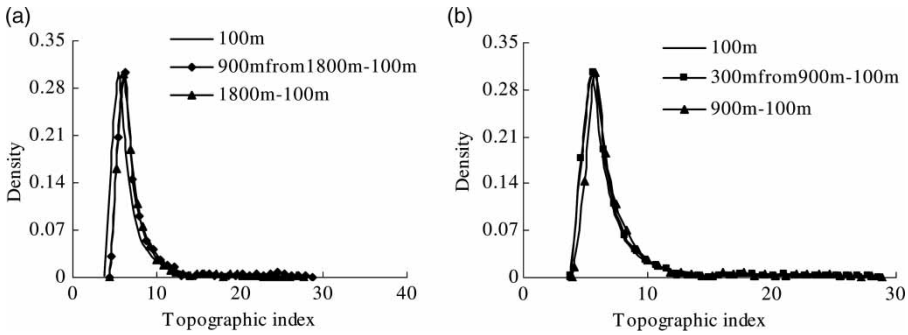

Figure 6 | Frequency curve of fractal slope with and without downscaling. (The meaning of '100 m', '900 m' and '300 from 900–100 m' are as in Figure 4. '900 m from 1,800–100 m' means the fractal slope at the target resolution of 100 m computed from the 900 m DEM which is downscaled from 1,800 m DEM.)

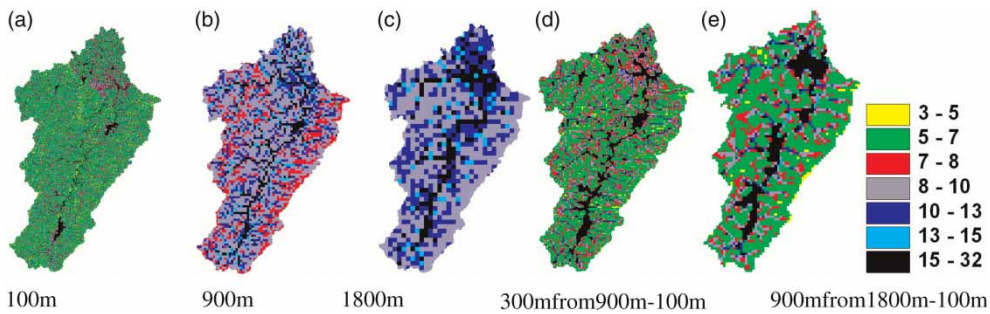

Figure 7 | Spatial distribution of topographic index and scaled topographic index at different DEM resolutions. (The meaning of '100 m', '900 m' and '300 from 900m-100 m' are as in Figure 4. '900 m from 1,800 m–100 m' means the fractal slope at the target resolution of 100 m computed from the 900 m DEM which is downscaled from 1,800 m DEM.)

From the previous analysis, the scaled topographic index distribution from disaggregated 300 and 900 m DEMs which originated from 900 and 1,800 m DEMs to 100 m DEM resolution are much closer to the distribution of topographic index at 100 m resolution DEM. The former is named FTI1, and the latter is named FTI2. Both of them were used in the streamflow simulation. Table 2 shows that the simulated runoff from the scale-invariant TOPMODEL applied at 900 and 1,800 m resolution DEM, with the same set of effective parameter values derived from 100 m resolution DEM, matches well with the simulated runoff of the 100 m DEM resolution TOPMODEL. This finding indicates that the parameter calibrated from finer DEM resolution TOPMODEL can be applied in the coarse DEM resolution TOPMODEL. The identified parameters are independent of DEM resolution by the utilization of the scale-invariant model.

The simulated hourly discharge hydrograph of FTI1 and FTI2 agrees well with that of 100 m DEM in Figure 8. Comparing the result with Figure 3, it can be concluded that the scale-invariant model can remove the partial effect of DEM resolution on hydrologic simulation.

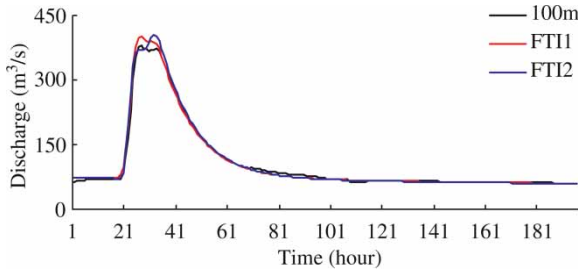

Figure 8 | Comparison of hourly discharge hydrograph of No. 800612 flood with different scaled topographic index.

CONCLUSION

Based on the downscaled DEM from the coarse-resolution DEM, this research has applied the concept of resolution factor to account for the effect of scale in upslope contributing area and a fractal method as an approach to account for the effect of scale on slopes, which are combined to develop the method to downscale topographic index distribution. This method can successfully derive higher resolution estimates of topographic characteristics at finer resolution DEM by using only a coarse-resolution DEM. The method to downscale the topographic index is then coupled with TOPMODEL to develop the scale-invariant TOPMODEL.

Table 2 | Comparison of simulation performance of 18 flood events using different scaled topographic index

Flood event	No.	Efficiency coefficient			Relative error of runoff depth (%)			Relative error of flood peak discharge (%)		
		100 m	FTI1	FTI2	100 m	FTI1	FTI2	100 m	FTI1	FTI2
Calibration	800504	0.92	0.83	0.90	−4.4	−3.8	−3.5	1.4	6.3	5.0
	800612	0.95	0.92	0.93	2.8	3.6	4.0	0	4.2	4.5
	810523	0.88	0.86	0.85	4.1	4.3	5.0	−0.1	0.7	1.9
	810622	0.93	0.92	0.93	0.1	0.5	0.7	0	1.3	1.4
	820509	0.84	0.85	0.82	−1.5	−1.1	−1.2	−0.1	1.0	1.6
	820531	0.93	0.95	0.95	7.6	7.6	8.0	0.2	3.8	3.4
	820608	0.91	0.92	0.91	6.0	6.5	6.6	−0.3	0.7	2.5
	820910	0.72	0.67	0.75	−6.1	−5.5	−4.7	−1.2	5.0	6.3
	840610	0.97	0.96	0.96	1.8	3.1	3.2	0	0.1	2.1
	840721	0.95	0.94	0.94	3.5	4.7	5.1	0	0	0.1
	850409	0.71	0.74	0.72	−1.8	−1.2	−1.3	1.1	1.0	1.7
	850428	0.91	0.89	0.89	−8.0	−7.8	−7.6	0.6	1.4	3.9
Validation	830502	0.94	0.93	0.92	5.0	5.2	5.2	−0.1	0.1	2.8
	830511	0.95	0.95	0.95	5.3	6.5	6.6	−0.1	4.1	3.8
	840416	0.94	0.91	0.91	0.6	0.6	1.0	0.1	1.8	2.9
	840511	0.84	0.86	0.88	6.5	5.7	4.5	0	0.4	0.2
	850523	0.94	0.94	0.95	8.3	8.2	8.7	−7.5	−7.4	−4.8
	850610	0.89	0.87	0.89	8.7	7.1	7.7	0	2.1	2.0

The scale-invariant TOPMODEL is independent of DEM resolution and can reduce the uncertainty result from the DEM resolution effects in hydrologic simulation. For further research, the reliability of the regression equations to predict fractal coefficient and fractal dimension should be improved, and a scientific method to determine the down-scaled resolution must be proposed.

REFERENCES

Barenblatt, G. I., Zhivago, A. V., Neprochnov, Y. P., Yu, P. & Ostrovskiy, A. A. 1984 The fractal dimension: a quantitative characteristic of ocean-bottom relief. *J. Oceanol.* **24**, 695–697.

Beven, K. & Kirkby, M. J. 1979 A physically based, variable contributing area model of basin hydrology. *Hydrol. Sci. Bull.* **24**, 43–69.

Fox, C. G. & Hayes, D. E. 1985 Quantitative methods for analysing the roughness of the seafloor. *Rev. Geophys.* **23** (1), 1–48.

Gallant, J. C. & Hutchinson, M. F. 1996 Towards an understanding of landscape scale and structure. In *Proc. Third International Conference/Workshop on Integrating GIS and Environmental Modeling*. National Center for Geographic Information and Analysis, Santa Barbara, CA.

Goodchild, M. F. 2001 Models of scale and scales of modeling. In: *Modelling Scale in Geographical Information Science* (N. J. Tate & P. M. Atkinson, eds.). Wiley, Chichester, pp. 3–10.

Huang, J. & Turcotte, D. L. 1989 Fractal mapping of digitized images: application to the topography of Arizona and comparisons with synthetic images. *J. Geophys. Res.* **94** (B6), 7491–7495.

Klinkenberg, B. 1992 Fractals and morphometric measures: is there a relationship? *Geomorphology* **5**, 5–20.

Klinkenberg, B. & Goodchild, M. F. 1992 The fractal properties of topography: a comparison of methods. *Earth Surface Process. Landforms* **17** (3), 217–234.

Martz, W. & Garbrecht, J. 1992 Numerical definition of drainage network and subcatchment areas from digital elevation models. *J. Comput. Geosci.* **18**, 747–761.

Pradhan, N. R., Tachikawa, Y. & Takara, K. 2004 A scale invariance model for spatial downscaling of topographic index in TOPMODEL. *Ann. J. Hydraul. Engng, JSCE* **48**, 109–114.

Pradhan, N. R., Tachikawa, Y. & Takara, K. 2006 A downscaling method of topographic index distribution for matching the scales of model application and parameter identification. *Hydrol. Process.* **20**, 1385–1405.

Quinn, P. F., Beven, K. J. & Lamb, R. 1995 The ln(α/tan β)index: how to calculate it and how to use it with the TOPMODEL framework. *Hydrol. Process.* **9**, 161–182.

Wolock, D. M. & Mccabe, G. J. 1995 Comparison of single and multiple flow direction algorithms for computing topographic parameters in TOPMODEL. *Water Resour. Res.* **31**, 1315–1324.

Wolock, D. M. & Price, C. V. 1994 Effects of digital elevation model map scale and data resolution on a topography based watershed model. *Water Resour. Res.* **30** (11), 3041–3052.

Wolock, D. M. & Mccabe, G. J. 2000 Differences in topographic characteristics computed from 100- and 1000-m resolution digital elevation model data. *Hydrol. Process.* **14**, 987–1002.

Xu, J., Ren, L. L., Cheng, Y. H. & Yuan, F. 2008 Topographic index calculation that is independent of the DEM spatial resolution. *J. Tsinghua Univ. (Sci&Tech)* **48** (6), 983–986.

Zhang, W. & Montgomery, D. R. 1994 Digital elevation model grid size, landscape representation, and hydrologic simulations. *Water Resour. Res.* **30**, 1019–1028.

Zhang, X., Drake, N. A., Wainwright, J. & Mulligan, M. 1999 Comparison of slope estimates from low resolution DEMs: scaling issues and a fractal method for their solution. *Earth Surface Process. Landforms* **24**, 763–779.

First received 8 October 2009; accepted in revised form 22 April 2010. Available online December 2011